

No. GH 33574A1. One of the authors (S. D. LeRoux) is grateful to the South African Atomic Energy Board for partial support of his stay at Purdue University.

<sup>1</sup>D. L. Spears, Phys. Rev. B 2, 1931 (1970); E. D. Palik and R. Bray, Phys. Rev. B 3, 3302 (1971).

<sup>2</sup>M. Yamada, C. Hamaguchi, K. Matsumoto, and J. Nakai, Phys. Rev. B 7, 2682 (1973); U. Gelbart and A. Many, Phys. Rev. B 7, 2713 (1973).

<sup>3</sup>R. Köhler, W. Möhling, and H. Peibst, Phys. Status Solidi 41, 75 (1970).

<sup>4</sup>B. E. Warren, *X-Ray Diffraction* (Addison-Wesley, Reading, Mass., 1969), Chap. 11.

<sup>5</sup>R. Köhler, W. Möhling, and H. Peibst, Phys. Status Solidi (b) 61, 439 (1974).

<sup>6</sup>D. G. Carlson, A. Segmüller, E. Mosekilde, H. Cole, and J. A. Armstrong, Appl. Phys. Lett. 18, 330 (1971).

<sup>7</sup>T. Ishibashi, M. Kitamura, and A. Odajima, Phys. Lett. 44A, 371 (1973).

<sup>8</sup>V. Dolat, J. B. Ross, and R. Bray, Appl. Phys. Lett. 13, 60 (1968); J. B. Ross, Ph.D thesis, Purdue University, 1972 (unpublished).

<sup>9</sup>H. N. Spector, Phys. Rev. 125, 1880 (1962), and 165, 562 (1968); K. P. Weller and T. Van Duzer, J. Appl.

Phys. 40, 4278 (1969); W. J. Fleming and J. E. Rowe, J. Appl. Phys. 42, 2041 (1971). The frequency of maximum acoustoelectric gain for small phonon intensity is given by  $f_m = (1/2\pi)(ne^2v_s^2/kT)^{1/2}$  when the condition  $q_m l / \mu B < 1$  applies, as is especially the case for the present experiment. ( $v_s$  is the fast-TA-phonon velocity, equal to  $2.3 \times 10^5$  cm/sec;  $q_m = 2\pi f_m / v_s$ , and  $l$  and  $\mu$  are the mean free path and mobility of the electrons.) The frequencies observed for the phonon satellite peaks will be generally somewhat lower than  $f_m$  because the frequency dependence of the lattice attenuation shifts the *net* gain downward (see Ref. 1). There can be further downshift with increasing phonon intensity [see T. E. Parker and R. Bray, Phys. Lett. 45A, 347 (1973)].

<sup>10</sup>General Electric No. 7031.

<sup>11</sup>R. Bray, IBM J. Res. Develop. 13, 487 (1969).

<sup>12</sup>Parker and Bray, Ref. 9.

<sup>13</sup>D. G. Carlson and A. Segmüller, Phys. Rev. Lett. 28, 175 (1972).

<sup>14</sup>H. Kroger, Appl. Phys. Lett. 4, 190 (1964); E. M. Conwell and A. K. Ganguly, Phys. Rev. B 4, 2535 (1971).

<sup>15</sup>B. W. Batterman, Phys. Rev. 127, 686 (1962).

## Van Hove Singularities of the Surface Phonon Density from Inelastic Reflection of Atoms\*

Giorgio Benedek

*Gruppo Nazionale de Struttura della Materia del Consiglio Nazionale delle Ricerche,  
Istituto di Fisica dell'Università, Milan, Italy*

(Received 19 February 1975)

The main peaks of the angular distribution of atoms inelastically reflected from a crystal surface are shown to be associated with analytical critical points of the surface phonon dispersion curves, particularly those of Rayleigh and Lucas modes. Because of such a relation, the frequencies and wave vectors of these modes could be measured by analyzing the shift of the peaks under a change of the angle of incidence.

Since the work by Cabrera, Celli, and Manson,<sup>1</sup> the inelastic reflection of atoms by crystal surfaces has been considered one of the most useful tools for investigating surface phonons. However, coupled high-resolution measurements of both velocity and angular distributions<sup>2</sup> are still severely limited by the actual low detection efficiencies. Williams and Mason,<sup>3,4</sup> through sophisticated measurements of the angular distribution of He and Ne scattered from LiF and NaF surfaces, were able to show that the sidebands observed around the elastic peaks correspond to one-phonon inelastic processes and, in some cases, can be associated with Rayleigh waves.

In this Letter I show that the main peaks of the inelastic angular distribution, observed under suitable experimental conditions, are related to analytical critical points of the surface dispersion curves, namely to Van Hove singularities of the surface density,<sup>5</sup> and particularly to those associated with Rayleigh and Lucas<sup>6</sup> modes.

The differential one-phonon reflection coefficient, at zero surface temperature and up to unitarity corrections, is given by<sup>7</sup>

$$\frac{d^2R^{(1)}}{d\omega d\Omega_f} = \frac{m^2 \alpha_c}{4\pi^2 \hbar^3} \frac{q_f}{q_{iz}} \sum_{\gamma\gamma'} Z_{\gamma'}^*(\vec{K}, \omega) Z_{\gamma}(\vec{K}, \omega) \rho_{\gamma\gamma'}(\vec{k}, \omega^2), \quad (1)$$

where  $\omega$  is the phonon frequency,  $\Omega_f$  the outgoing-beam solid angle,  $m$  the particle mass,  $\alpha_c$  the surface unit-cell area,  $\vec{q}_i = (\vec{K}_i, q_{iz})$  and  $\vec{q}_f = (\vec{K}_f, q_{fz})$  the wave vectors of incoming and outgoing particles,

and  $\hbar\vec{K} = \hbar(\vec{K}_i - \vec{K}_r)$  the surface momentum transfer;  $\vec{K} = \vec{k} + \vec{G}$ , where  $\vec{k}$  is the phonon wave vector and  $\vec{G}$  a surface reciprocal vector. The matrix elements of the surface-projected phonon density  $\rho(\vec{K}, \omega^2)$  and the components of the coupling "forces"  $Z$  are defined in Ref. 7.

For planar scattering, the energy loss  $\hbar\omega$  is related to the momentum transfer by the kinematical equation

$$\omega/\omega_i = 1 - (1 - K/K_i)^2 \sin^2\theta_i/\sin^2\theta_f, \quad (2)$$

$K$  and  $K_i$  being the components of  $\vec{K}$  and  $\vec{K}_i$  on the incidence plane;  $\theta_i$  and  $\theta_f$  are the angles of incidence and reflection, respectively, and  $\hbar\omega_i \equiv E_i = \hbar^2 q_i^2/2m$  the incident particle energy. The angular distribution function

$$I(\theta_f) = \int d\omega (d^2R^{(1)}/d\omega d\Omega_f) \quad (3)$$

is obtained by a line integration in the plane  $(K, \omega)$  along the parabola represented by Eq. (2).

The differential reflection coefficient displays the structure of  $\rho(\vec{K}, \omega^2)$ , namely, a superposition of the continuous spectrum associated with the bands of bulk phonons projected onto the surface, and a discrete spectrum formed by a few  $\delta$  functions located at the frequencies of surface and pseudosurface modes.

According to the analysis reported in a previous work,<sup>7</sup> the coefficients  $Z_\gamma(\vec{K}, \omega)$  for the scattering of *neutral* particles introduce an enhancement in the response of acoustic phonons (mainly Rayleigh modes) and a dramatic cutoff in the optical region. Usually, only the lowest optical surface mode, the sagittally polarized Lucas mode,<sup>8</sup> survives, giving an appreciable contribution, particularly at the border of the surface Brillouin zone.<sup>8</sup>

We focus our attention on the contribution to  $I(\theta_f)$  of surface localized modes, i.e. Rayleigh and Lucas modes. For these modes we have a term like

$$d^2R^{(1)}/d\omega d\Omega_f = A(K)\delta(\omega - \omega_s(K)), \quad (4)$$

$$I(\theta_f) \cong \bar{v}_s A(\vec{K}) [(\omega_i - \bar{\omega}_s)(\bar{\omega}_s - \bar{\omega})(\theta_f - \bar{\theta}_f) \cot \bar{\theta}_f]^{-1/2}, \quad (6)$$

where  $\bar{\omega} = v_s/(\vec{K} - K_i)$  is the second derivative of  $\omega$  with respect to  $K$  in Eq. (2) for  $K = \vec{K}$ .  $I(\theta_f)$  exhibits a typical inverse-square-root singularity at the left or at the right of  $\theta_f$ , depending on whether  $\bar{\omega}_s < \bar{\omega}$  or  $\bar{\omega}_s > \bar{\omega}$ . At large  $\theta_f$  the inelastic singularities become more and more important, because of the factor  $\cot^{-1/2}\bar{\theta}_f$ . It is important to remark that for beams of atoms at thermal energies and for large incidence and reflectance angles (e.g.,  $\theta_i$  and  $\theta_f > 45^\circ$  in the case of Ne),  $\bar{v}_s$  is much smaller than ordinary phonon phase velocities  $\omega/k$ . This means that the tangency points are very close to the analytical critical points ( $\partial\omega/\partial k = 0$ ) of the phonon dispersion curves. Under these conditions the main peaks of the

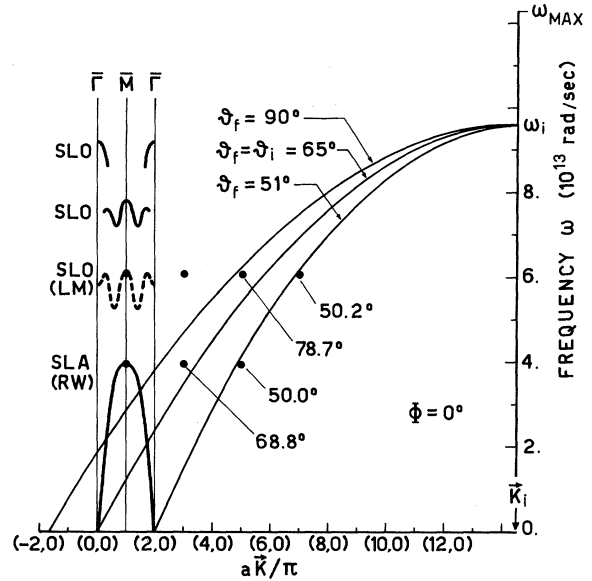


FIG. 1. Energy loss versus momentum transfer and surface phonon dispersion curves for planar scattering of Ne from LiF (001) surface [incidence plane parallel to (100);  $\theta_i = 65^\circ$ ,  $E_i = 18 \times 10^{-14}$  erg, according to experiments of Ref. 9]. Solid circles refer to the Rayleigh surface mode (RW) and the Lucas pseudosurface mode (LM) at the  $\bar{M}$  point of the surface Brillouin zone. The  $\theta_f$  values of the parabolas crossing these points are indicated and give approximately the location of singularities in the angular distribution.

where  $\omega_s(K)$  is the dispersion function for one of the above surface modes. This term contributes to  $I(\theta_f)$  when the parabola, Eq. (2), for  $\theta_f$  has some intersection with the dispersion curve  $\omega = \omega_s(K)$ . When the two curves are tangent,  $I(\theta_f)$  becomes singular. By calling  $\vec{K}$  and  $\bar{\omega}$  the wave vector and the frequency corresponding to a tangency point, and  $\bar{\theta}_f$  the related angle [via Eq. (2)], and by expanding  $\omega_s(K)$  around  $\vec{K}$ ,

$$\omega_s(K) = \bar{\omega}_s + (K - \vec{K})\bar{v}_s + \frac{1}{2}(K - \vec{K})^2\bar{w}_s + \dots, \quad (5)$$

we can calculate the singular part of  $I(\theta_f)$  around  $\bar{\theta}_f$ . We obtain

angular distribution correspond to Van Hove singularities of the surface phonon density. Notice that the Van Hove singularities in two dimensions are stepwise for minima or maxima, and logarithmic for saddle points in the constant-energy surface,<sup>5</sup> while the line integration yields the appearance of one-dimensional inverse-square-root singularities. As a consequence, the angular distributions show "amplified" Van Hove singularities.

In Fig. 1, the parabolas for Ne scattered by the (001) surface of LiF in the plane parallel to the (100) axis, and for  $\theta_i = 65^\circ$ , are plotted for some values of  $\theta_f$ , and superimposed onto the surface phonon dispersion curves of LiF (reproduced only in the first Brillouin zone).<sup>7</sup> According to the above arguments, the relevant phonons are Rayleigh (RW) and Lucas (LM) modes at the  $\bar{M}$  point (solid circles); singularities are expected for the values of  $\theta_f$  indicated at each solid circle.

This simple analysis is confirmed by the comparison of the calculated angular distribution of Ne scattered from LiF for  $\theta_i = 65^\circ$  and  $50^\circ$  with the experimental results of Boato and Cantini<sup>9</sup> (Fig. 2). A Green's-function method and breathing shell model were used for surface dynamics. The coefficient  $d^2R^{(1)}/d\omega d\Omega_f$  was calculated as in Ref. 7, in the framework of the distorted-wave Born approximation (DWBA). One could argue that, for the case of Ne atoms scattered from LiF, a semiclassical approach should be preferred to DWBA. The choice of DWBA is justified by the simple form taken by  $Z_\gamma(\vec{k}, \omega)$ ,<sup>7</sup> as well as by the weak influence of the scattering model on the calculated angular distribution, whose shape is mainly determined by the phonon structure. For simplicity, I have neglected also the  $\vec{G}$  dependence of  $Z_\gamma$ . Except for a few discrepancies,<sup>10</sup> the correspondence between experimental and theoretical structures is good; particularly, the RW singularities are closely associated with important experimental peaks (labeled by  $\rho$ ).

The LM singularities, derived from the theoretical frequency  $\omega_{LM}(\bar{M}) = 6.15 \times 10^{13} \text{ sec}^{-1}$ , could be associated either with the peaks  $\lambda$  [corresponding to  $\omega_{LM}(\bar{M}) = 6.09$ ] or with  $\lambda'$  [corresponding to  $\omega_{LM}(\bar{M}) = 6.23 \times 10^{13} \text{ sec}^{-1}$ ]. At present, both interpretations are acceptable, the theoretical  $\omega_{LM}(\bar{M})$  being reliable with an error of some percent.

From the above considerations it turns out that combining two or more experimental angular distributions taken at different incidence angles en-

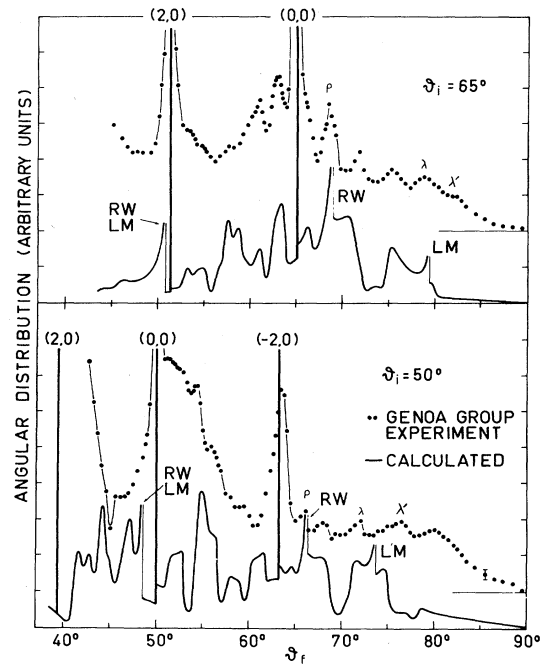


FIG. 2. Calculated inelastic angular distributions of Ne from LiF (001) surface for  $\theta_i = 65^\circ$  and  $50^\circ$  compared with experimental data of Boato and Cantini (Ref. 9). The experimental elastic peaks correspond to  $\theta$  functions in the calculated spectra.

ables one to obtain the frequency and the wave vector of some relevant phonons localized at the surface. For this purpose, the peaks associated with these surface phonons can be distinguished from the band contributions by measuring their shift  $d\theta_f$  under a change in the incidence angle  $d\theta_i$ . From the relation [deduced by differentiating Eq. (2)]

$$d \ln \sin \bar{\theta}_f / d \ln \sin \theta_i = K_i / (K_i - \bar{K}),$$

one obtains  $\bar{K}$ , and hence the frequency  $\bar{\omega}$ , via Eq. (2).

The author acknowledges the kind hospitality enjoyed at the International Center for Theoretical Solid State Physics at the University of Liège, in the framework of the ESIS project. Many thanks to Professor G. Boato and his Genoa group co-workers for several useful discussions and for having supplied the detailed experimental data.

\*Work performed in the framework of the joint project ESIS (Electron Structure In Solids) of the University of Antwerpen and the University of Liège, Belgium.

<sup>1</sup>N. Cabrera, V. Celli, and R. Manson, *Phys. Rev. Lett.* **22**, 346 (1969).

<sup>2</sup>S. S. Fisher and J. R. Bledsoe, *J. Vac. Sci. Technol.* **9**, 814 (1972).

<sup>3</sup>B. R. Williams, *J. Chem. Phys.* **55**, 1315, 3220 (1971).

<sup>4</sup>B. F. Mason and B. R. Williams, *J. Chem. Phys.* **61**, 2765 (1974).

<sup>5</sup>A. A. Maradudin, E. W. Montroll, and G. H. Weiss, in *Theory of Lattice Dynamics in the Harmonic Approximation*, Suppl. No. 3 to *Solid State Physics*, edited by H. Ehrenreich, F. Seitz, and D. Turnbull (Academic, New York, 1963), Chap. III.

<sup>6</sup>A. A. Lucas, *J. Chem. Phys.* **48**, 3156 (1968).

<sup>7</sup>G. Benedek and G. Seriani, *Jpn. J. Appl. Phys.*, Suppl. No. 2, Pt. 2, 545 (1974).

<sup>8</sup>In LiF the sagittal Lucas mode is a broad resonant mode all over the surface Brillouin zone, except at the symmetry points  $\bar{\Gamma}$ ,  $\bar{M}$ , and  $\bar{X}$  where it becomes a pseudo-

surface mode. The contribution of  $\bar{\Gamma}$  Lucas modes is negligible because a neutral particle is unable to excite purely optical modes.

<sup>9</sup>G. Boato and P. Cantini, *Jpn. J. Appl. Phys. Suppl.* No. 2, Pt. 2, 553 (1974).

<sup>10</sup>The integral of Eq. (3) has been performed for the band modes over a mesh of sixteen bins for each  $\bar{\Gamma}\bar{M}\bar{\Gamma}$  interval. The local-mode singular contributions have been calculated analytically from Eq. (6) and added. Because of quite long computer times needed in calculating  $Z_\gamma$  and  $\rho$ , I could not use a thicker mesh, which limits the accuracy of the present results. The possible water contamination of the surface would affect the experimental data [see, e.g., D. E. Houston and D. R. Frankl, *Phys. Rev. Lett.* **31**, 298 (1973)], making the comparison with calculation questionable. However, a recent work by Wilsch *et al.* (unpublished) gives definitive evidence that the standard preparation procedure gives water-free surfaces.

## Effect of <sup>3</sup>He Impurities on the Lifetime of Ions Trapped on Quantized Vortex Lines\*

Gary A. Williams† and Richard E. Packard

*University of California, Berkeley, California 94720*

(Received 5 May 1975)

The lifetimes of both positive and negative ions trapped on quantized vortex lines in rotating <sup>3</sup>He-<sup>4</sup>He mixtures have been measured at temperatures down to 0.1 K. Evidence is found that the <sup>3</sup>He condenses at the vortex core, and possibly at the surface of the electron bubble.

This Letter briefly describes recent measurements of the trapped lifetimes of positive and negative ions bound to quantized vortex lines in <sup>3</sup>He-<sup>4</sup>He mixtures.<sup>1</sup> The primary purpose of these measurements was to see if the trapped lifetime would exhibit effects attributable to <sup>3</sup>He condensing either in the vortex core<sup>2,3</sup> or on the surface of the ions.<sup>4</sup>

In pure liquid <sup>4</sup>He it is widely believed that the negative ion is an electron self-trapped in a bubble with radius of 17 Å.<sup>5</sup> The positive ion is thought to be a singly ionized He atom surrounded by an electrostrictively induced solid "snowball" with a radius of approximately 6 Å. When either of these ions is near a quantized vortex line they feel attracted to the line as a result of the Bernoulli pressure. The ion can become localized in a hydrodynamic potential well centered on the line. The average length of time for which the ion remains trapped (trapped lifetime) depends on a Boltzmann factor containing the well depth and on an attempt frequency which depends on the de-

tailed motion of the ion in the well.<sup>6</sup> Thus the intrinsic trapped half-life  $\tau_{1/2}$  can be written as

$$\tau_{1/2} = \tau_0 e^{U/kT}, \quad (1)$$

where  $U$  represents the well depth,  $k$  is Boltzmann's constant,  $T$  is the temperature, and  $\tau_0^{-1}$  is the escape attempt frequency.

In addition to thermal escape, trapped ions can leave the fluid whenever a vortex line migrates to a wall and is destroyed, releasing its trapped charge.<sup>7</sup> This geometry-dependent mechanism determines the upper limit of the lifetime observed in a given experiment at low temperatures.

If <sup>3</sup>He is present in the superfluid it can profoundly influence the lifetime. If the <sup>3</sup>He condenses on the vortex core it will decrease the well depth  $U$  and may also change  $\tau_0$ . Furthermore if the <sup>3</sup>He changes the size of the ion it will change both  $U$  and  $\tau_0$ . Since  $\tau_{1/2}$  depends strongly on  $U$  and  $\tau_0$ , lifetime measurements provide a sensitive probe of these parameters.